Detection of NO₂ down to ppb Levels Using Individual and Multiple In₂O₃ Nanowire Devices

Daihua Zhang, Zuqin Liu, Chao Li, Tao Tang, Xiaolei Liu, Song Han, Bo Lei, and Chongwu Zhou*

Department of E.E.-Electrophysics, University of Southern California, Los Angeles, California 90089

ABSTRACT

We demonstrate detection of NO₂ down to ppb levels using transistors based on both single and multiple In₂O₃ nanowires operating at room temperature. This represents orders-of-magnitude improvement over previously reported metal oxide film or nanowire/nanobelt sensors. A comparison between the single and multiple nanowire sensors reveals that the latter have numerous advantages in terms of great reliability, high sensitivity, and simplicity in fabrication. Furthermore, selective detection of NO₂ can be readily achieved with multiple-nanowire sensors even with other common chemicals such as NH₃, O₂, CO, and H₂ around.

Chemical sensing based on various nanostructures[1−11] has attracted enormous attention, as this is widely perceived as one of the most promising areas for nanotechnology to generate significant impact. Among the chemicals studied, NO₂ is one of the most dangerous air pollutants, which plays a major role in the formation of ozone and acid rain. Continued or frequent exposure to NO₂ concentrations higher than the air quality standard (53 ppb) may cause increased incidence of acute respiratory illness in children.[12] The detection and measurement of NO₂ gas are thus of great importance in both environmental protection and human health. Solid-state sensors for NO₂ detection have been under development based on both conventional metal oxide thin films and one-dimensional nanostructures, however, with various limitations. For instance, most existing metal oxide thin-film sensors work at elevated temperatures with sensing limitations around 1 ppm or even higher.[13−17] Nanowires or nanobelts made of metal oxides can deliver better performance because of their enhanced surface-to-volume ratios, and SnO₂ nanobelts have been demonstrated to detect 3 ppm NO₂ at room temperature.[5] In addition, by operating SnO₂ nanobelt sensors at 400 °C, detection down to 0.5 ppm NO₂ has been successfully achieved.[7] These represent significant advance in the field of solid-state chemical sensing; however, the detection limit does not satisfy the requirement of 53 ppb NO₂ set by the U.S. Environmental Control Agency. On the other hand, carbon nanotube mat samples have been reported to reliably detect NO₂ down to 1 ppb or less, with the aid of functional polymer coating to enhance the sticking coefficient.[3]

In this letter we report the detection of NO₂ down to ppb levels for the first time with metal oxide nanowire transistors. Two types of devices have been studied based on both single and multiple In₂O₃ nanowires operating at room temperature and without the help of functional polymer coating. This represents orders-of-magnitude improvement over previously reported metal oxide film or nanowire/nanobelt sensors, and rivals the performance of the best nanotube chemical sensors. While single In₂O₃ nanowire devices exhibited strong gate dependence and nice transistor behavior, sensors based on multiple In₂O₃ nanowires displayed numerous advantages in terms of great reliability, high sensitivity down to 5 ppb, and simplicity in fabrication. Furthermore, selective detection of NO₂ among other common chemicals has been observed with multiple-nanowire sensors without the extra step of polymer coating. These novel devices are a proven new generation of NO₂ sensors that could replace the conventional devices, and even surpass the carbon nanotube (CNT) NO₂ sensors[2,3] in terms of their great simplicity in device fabrication.

In₂O₃ nanowires were synthesized by a laser ablation method, and details can be found in our previous publication.[18] This method typically produced single-crystalline In₂O₃ nanowires with diameters ∼10 nm and lengths ∼5 μm. These nanowires are wide band gap semiconductors with bixbyte crystal structure, as shown in Figure 1a. The conductance of In₂O₃ nanowires is directly related to the carrier concentration inside, which in turn can be altered by

---

* Corresponding author. E-mail: chongwuz@usc.edu.
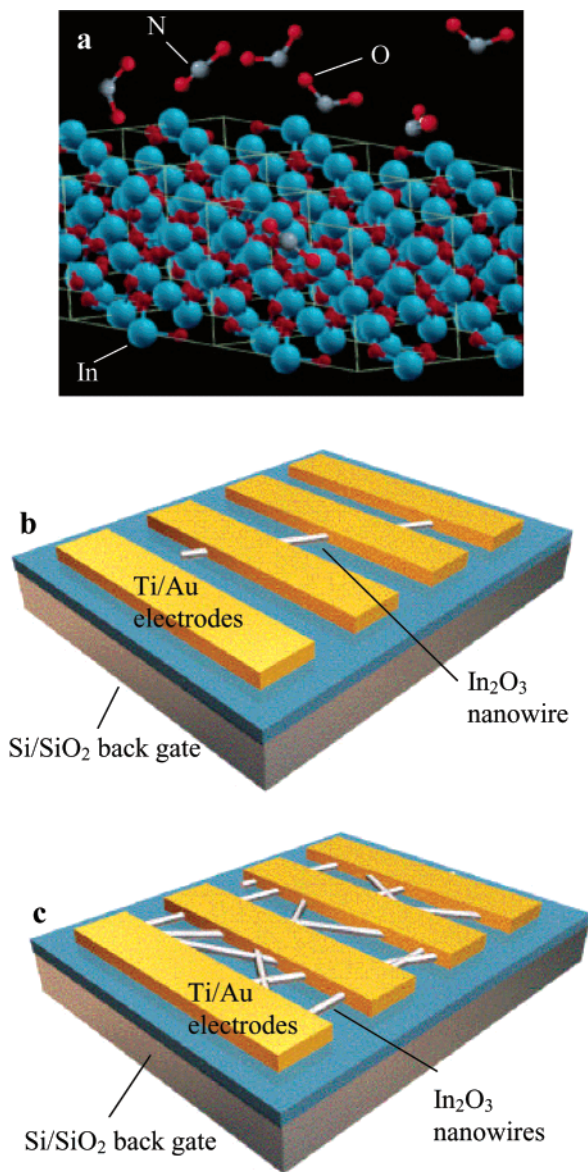
Figure 1. (a) Schematic view of the crystal lattice of the nanowire surface layer [(001) plane] and the surrounding NO_2 molecules. Red, blue, and gray spheres respectively represent oxygen, indium, and nitrogen atoms. (b) Single nanowire transistor structure, where Ti/Au are deposited on nanowire-decorated Si/SiO_2 substrate as drain and source electrodes. (c) Schematic of a multiwire device.

the adsorbed NO_2 molecules due to their strong electron-withdrawing capability. For the fabrication of single nanowire devices, In_2O_3 nanowires were first sonicated into a suspension and then deposited onto degenerately doped Si wafers covered with 500 nm SiO_2. Finger-shaped metal electrodes were then patterned and deposited using photolithography and electron beam evaporation. Figure 1b shows a schematic drawing of the nanowire transistor structure. The density of the dispersed In_2O_3 nanowires is optimized to yield many devices connected with a single nanowire. The silicon substrate was used as a back gate while the metal contacts worked as the source and drain electrodes. The devices were mounted in a sealed chamber with electrical feedthrough and gas inlet/outlet. Compared to our previous work using a stainless steel cross of one inch in diameter,[6] this study used
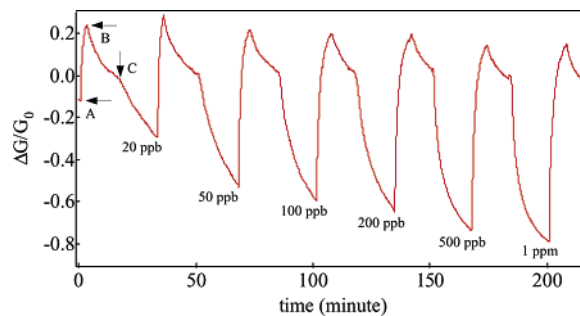
Figure 2. Sensing response of a single nanowire device to NO_2 diluted in air. The normalized conductance change ($\Delta G/G_0$) is plotted as a function of time with the nanowire sensor exposed to NO_2 of various concentrations. Recovery was made by UV light (254 nm) desorption of NO_2.

a one-inch through tube, and the dead volume was therefore minimized. Sensing experiments were carried on by monitoring the single nanowire conductance under different NO_2 concentrations.

Figure 2 plots the change in nanowire conductance normalized by initial conductance (G_0) at gate bias $V_g = 0$ V as a function of time. Six cycles were successively recorded, corresponding to six different NO_2/air concentrations ranging from 20 ppb to 1 ppm, respectively. The device recovery was realized by desorbing NO_2 molecules with ultraviolet (UV) light illumination (at point A, taking the first cycle as an example). The nanowire conductance kept rising until the UV light was turned off at point B. Due to electron−hole recombination and readsorption of O_2 and H_2O in the air, the conductance decreased gradually with the decreasing carrier concentration in the nanowire. Diluted NO_2 gas (NO_2 mixed with air, 20 ppb) was introduced to the airflow at point C, before a fully stabilized state was reached. The NO_2 molecules, known as strong electron-withdrawing groups, further reduced the electron density along the nanowire, leading to a higher dropping rate of the conductance. The effect of NO_2 was clearly demonstrated by the slope alteration at C. The normalized conductance change (S) for 20 ppb NO_2 was estimated as 25% with the definition $S = \Delta G/G_0 = (G - G_0)/G_0$, where G and G_0 denote the nanowire conductance before and after 20 minute NO_2 exposure. The minimum detectable NO_2 concentration was found to be ~20 ppb NO_2 in air, where a slope modification at the exposure point can still be distinguished but tends to vanish at lower concentrations. With higher concentration NO_2 used, more pronounced conductance modulation was observed, as shown in Figure 2. Eight single In_2O_3 nanowire transistors were studied and similar performance was consistently obtained in terms of the normalized conductance change, response time, and detection limits. Control measurements have also been carried out with pure Ar replacing the compressed air as the diluting gas, to verify the influence of O_2 and moisture in the air. O_2 and moisture are known as oxidization groups for In_2O_3, with the similar, but much weaker, electron withdrawing function compared to NO_2. We have found that the detection limit can be pushed further to ~5 ppb NO_2 when Ar instead of air was used (result not shown).
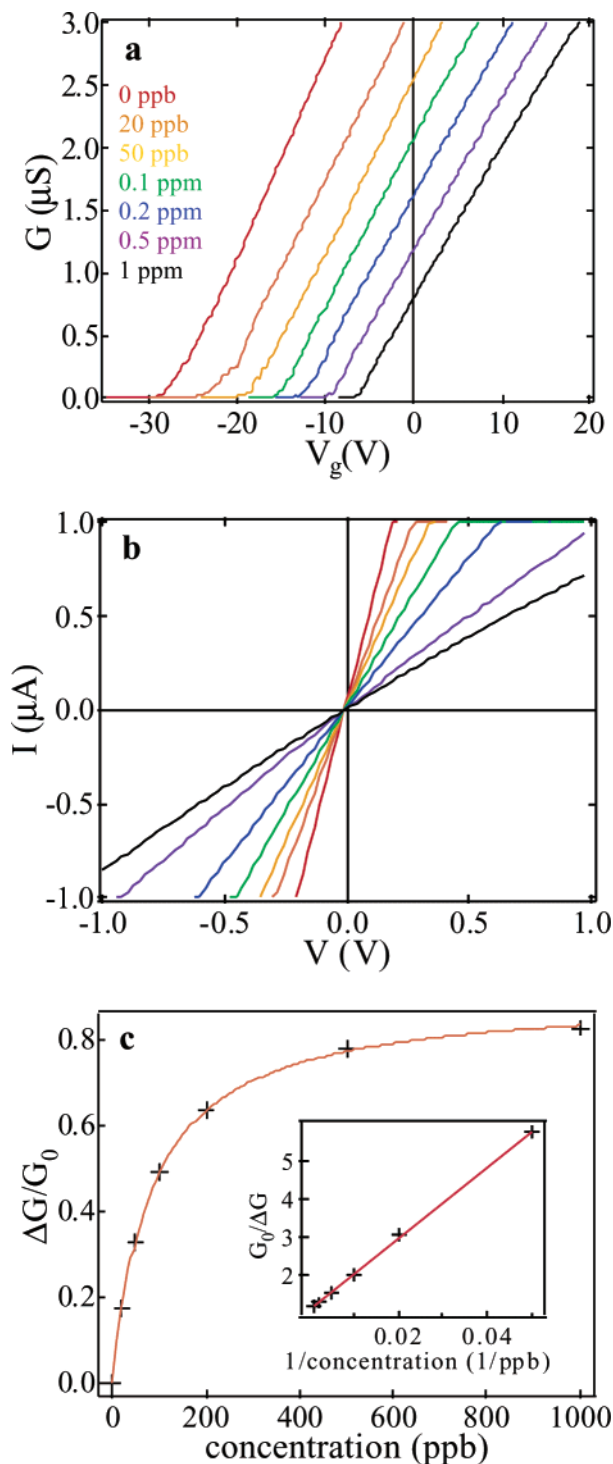
Figure 3. (a) $I-V_g$ curves for the device recorded after exposure to NO_2 of successively increasing concentrations. Curves (from left to right) correspond to NO_2 concentrations of 0, 20, 50, 100, 200, 500, and 1000 ppb, respectively. (b) $I-V$ curves taken in the seven different NO_2 concentrations. (c) Normalized conductance change $S = \Delta G/G_0$ vs NO_2 concentrations C, which was fitted using $S = 1/(A + B/C)$. Inset: $1/S$ vs $1/C$ with a linear line fit.

Figure 3a shows the conductance (G) vs gate bias (V_g) curves recorded in the six different NO_2 concentrations after exposure for 20 min. A $G-V_g$ curve taken at the initial state (at point C in Figure 2) was also plotted as a reference. The threshold gate voltage shifted rightward monotonically with

the increasing NO_2/air concentration, implying the gradually suppressed carrier concentration inside the nanowire that scales linearly with the absolute value of gate threshold. The Au/Ti/In_2O_3 contact has been proven a very transparent Schottky barrier by systematic 2- and 4- probe $I-V$ measurements (result not shown). Figure 3b displays the current−voltage ($I-V$) curves (at $V_g = 0$ V) obtained under the six different NO_2 concentrations used. The conductance of the device was monotonically suppressed with increasing NO_2 concentration, from 4.5 μS before the exposure to 0.7 μS with 1 ppm NO_2. These curves are found to be rather linear and indicate the Ohmic contact nature for the sensing devices in diluted NO_2 environments. It can be therefore concluded that the NO_2 molecules modify the sensor conductance mostly by means of tuning the electron density (Fermi energy) inside the nanowire, with negligible contribution from the band shape modulation at the electrode contacts. The slopes of the $G-V_g$ curves, which reflect the carrier mobility and transistor sub-threshold values, thus remain basically unaltered in different NO_2 concentrations, as demonstrated by the parallel feature of the curves in Figure 3a. Figure 3c plots the derived normalized sensors response as a function of NO_2 concentrations (C). The curve is rather linear at low concentrations, but tended to saturate when the NO_2 partial pressure went up. This curve can be well fitted with the following equation:

$$S = \frac{A}{1 + \dfrac{B}{C}}$$

with $A = 0.8954$ and $B = 83.45$, which has also been further confirmed by the linear fitting of S^{-1} vs C^{-1} shown in Figure 3c inset. This can be understood as the surface coverage of adsorbed molecules follows Langmuir isotherm.[3,19] At lower concentrations (<100 ppb in our case), eq 1 can be simplified into a linear relation $S = (A/B)\cdot C$, and thus the devices exhibited a linear dependence between the normalized sensor response and the NO_2 concentration. At higher concentrations, the surface coverage tends to saturate and hence leads to the saturated response observed in Figure 3c.

The above results and analyses have summarized the outstanding detection ability of the single In_2O_3 nanowire transistors. However, the fabrication of such devices relies on a fortuitous process to obtain devices connected with single nanowires. For cost-conscious chemical sensing applications, it is of utmost importance to develop a process involving minimal fabrication steps and yet producing high-quality devices with a yield approaching 100%. Furthermore, as reported before,[6] single In_2O_3 nanowire devices also respond to the presence of NH_3 in addition to NO_2. It is therefore important to develop reliable nanowire sensors that can selectively respond to NO_2. Our approach to solve the above-mentioned problems is to fabricate and exploit multiple-nanowire devices, similar to the approach adopted by carbon nanotube sensors,[3,4] and NO_2 sensors based on tin oxide two-dimensional nanostructures.[20] This technique boasts numerous advantages such as simplified fabrication, a perfect yield ~100%, enhanced sensitivity, and more interestingly, selec-

tive response to NO$_2$. The multiwire device fabrication started directly with Si/SiO$_2$ substrates that were used to collect the products during the nanowire synthesis. After the synthesis, these substrates hosted abundant In$_2$O$_3$ nanowires distributed uniformly across the surface. As discussed in our previous reports,[18] the concentration of the grown In$_2$O$_3$ nanowires is determined by the catalytic particle density, therefore desired device conductance could be obtained by simply tuning the catalyst concentration on the Si/SiO$_2$ substrates. Standard photolithography and metal deposition were then carried out to pattern finger-like electrodes across the substrate, yielding devices with multiple nanowire connections shown in Figure 1c. Since the nanowires disperse on the substrate in a rather uniform manner, the as-fabricated devices are expected to possess similar and consistent characteristics, e.g. conductance, threshold gate voltage and sensitivity, etc. With only one step of photolithography and metallization, the fabrication of such multiwire devices owns apparent advantage in terms of its great simplicity over that of the multiple CNT sensors,[2,3] where many sequential fabrication steps are required to put down alignment marks, pattern the catalyst, and then form the metal electrodes. More importantly, this simple process, serving as a general fabrication template for most electronic noses built on 1D nanostructures, can be readily applied to all types of nanowires/nanobelts grown on solid substrates via thermal CVD and other synthesis techniques.

A typical SEM image taken with one of the as-fabricated multiwire sensors was shown in Figure 4a. The typical number of nanowires bridging adjacent metal electrodes is estimated to be 100~200. $I-V$ curves of the device were recorded while sweeping the gate voltage from 0 to −40 V with a step of 10 V, as plotted in Figure 4b. With substantially increased current channels, the multiwire transistor showed greatly enhanced conductance of 0.5 mS at $V_g = 0$ V, which is 2−3 orders higher than the average conductance of the single-wire devices. It was found that the sensitivity to electrostatic gating was significantly suppressed in the multiwire transistors. This can be clearly observed in the $I-V_g$ curve shown in the lower inset in Figure 4b, where only a ~40% change in device conductance was observed when V_g was swept from 0 to −40 V. The reduced gating effect stems from the fact that each multiwire device consisted of a large number of In$_2$O$_3$ nanowires often lying atop each other, and the gate dependence is therefore weakened due to the increased average gate-nanowire distance. This effect actually works to our advantage for chemical sensing purpose by rendering devices with high stability, as discussed below. In addition, these multiwire devices exhibited interesting features in many other aspects. Electrical probing of the sensor arrays revealed a device yield of 100%. In the upper inset of Figure 4b, we draw a histogram of the device conductance, which is based on statistics over randomly selected 50 devices from three different device chips. The sharp distribution clearly demonstrates the high consistency of the multiwire sensors.

In addition to the improved device yield, we have observed that these multiple nanowire devices offered even better
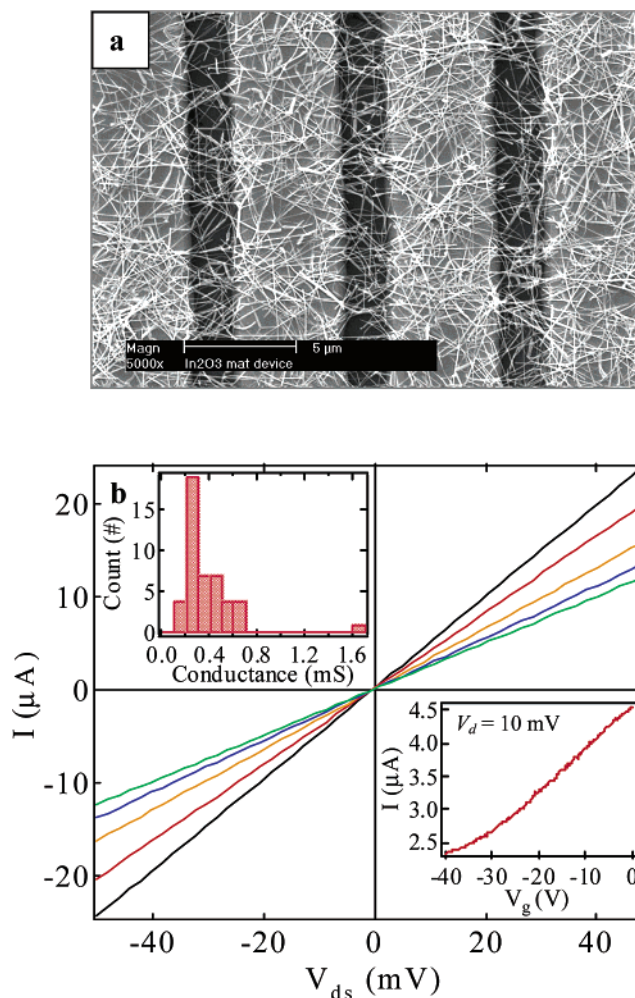
Figure 4. (a) SEM image of the as-fabricated multiwire devices, where bulk quantities ($10^2\sim10^3$) of In$_2$O$_3$ nanowires are contacted by four electrodes. (b) $I-V$ curves for the multiwire transistor recorded at five different gate voltages ($V_g = 0$, −10, −20, −30, and −40 V). The $I-V_g$ plot was shown in the lower-right inset. The upper-left inset presents a histogram of the multiwire device conductance, which was based on statistics over randomly selected 50 devices on three different chips.

sensitivity to NO$_2$ than the individual nanowire devices. Similar to the measurement we did in Figure 2, we recorded six sensing cycles in Figure 5a with the multiwire device, corresponding to NO$_2$/air concentrations of 5, 10, 20, 50, 100, and 200 ppb, respectively. The multiwire sensor showed an even lower detection limit of 5 ppb, compared to the 20 ppb limit of single nanowire sensors. Detailed examination showed a normalized conductance change of ~20% to 5 ppb NO$_2$ in air, with a response time of ~1000 s, defined as the time corresponding to a decrease of the resistance down to 80% of the original value. This room temperature detection limit is the lowest level so far achieved with all metal oxide film or nanowire sensors. We tentatively attribute this improved sensitivity to the formation of nanowire/nanowire junctions between the metal electrodes, a feature available in the multiple nanowire devices (Figure 4a) but missing in the single nanowire devices. Such junctions, when exposed to NO$_2$, should form a depleted layer around the intersection
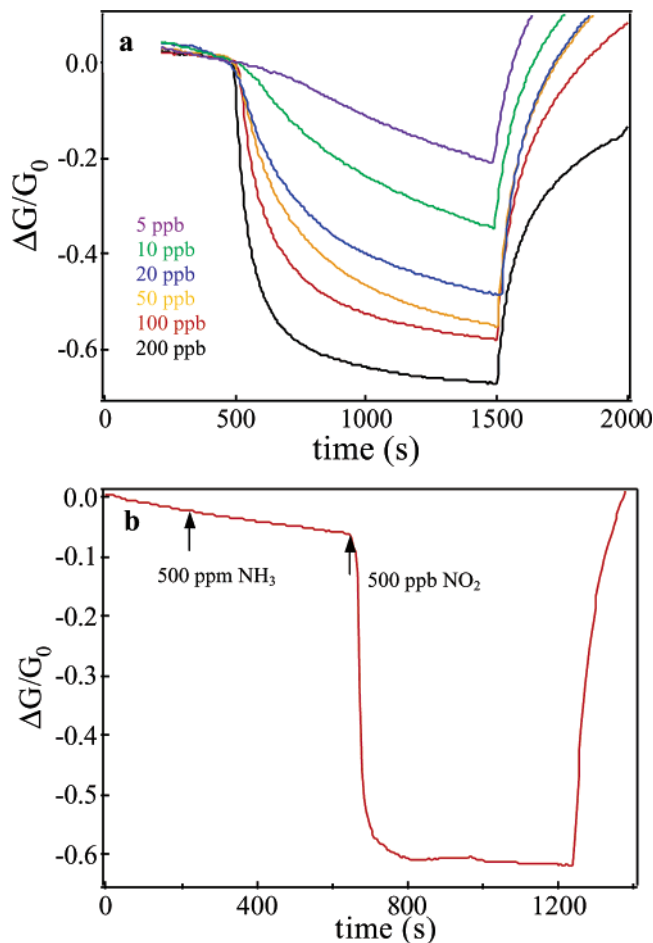
Figure 5. (a) Six sensing cycles of the multiwire device, corresponding to NO_2 concentrations of 5, 10, 20, 50, 100, and 200 ppb. (b) Selective sensing to NH_3 and NO_2 of the multiwire sensors. 500 ppm NH_3 and 500 NO_2 were introduced to the environment at $t = 200$ s and $t = 600$ s, respectively.

and thus block the electron flow in a way more prominent than the surface depletion of single nanowires with metal contacts.

In the last part of this report, we present our investigation on the selectivity of the multiwire sensors for detection of NO_2 against NH_3, which is another gas commonly used for chemical sensing studies. A sensing cycle to two gas species was recorded in Figure 5b, while 500 ppm NH_3 and 500 ppb NO_2 were succesively introduced to the environment. As clearly illustrated in the figure, no response was observed in the multiwire sensor upon exposure to 500 ppm NH_3 at $t = 200$ s. In sharp contrast, the sensor showed a pronounced response to 0.5 ppm NO_2, where the device conductance dropped instantly at the exposure time ($t = 600$ s). Such selective response to NO_2 and NH_3 was collectively exhibited by all the 10 measured multiwire devices on three different chips, but surprisingly, similar selectivity has been rarely seen in the single In_2O_3 nanowire sensors. We suggest an "ensemble-averaging effect" as one possible reason for the observed high selectivity in the multiwire sensors. In the previous study,[21] we have found that individual In_2O_3 nanowires with different oxygen vacancy doping concentrations could exhibit conductance change in opposite directions

upon exposure to NH_3. Accordingly, a large ensemble of In_2O_3 nanowires, with an appropriate doping level distribution, could have two opposite sensing responses canceling out each other and resulting in the immunity to NH_3. This unique property of In_2O_3 nanowire offers a new way to achieve selectivity, as compared to the conventional technique of using permeable polymer coatings.[2] We have tested detection of NO_2 among other common gases such as O_2, CO, and H_2 using the multiple nanowire devices, and selective response to NO_2 was also observed. Nevertheless, we note that this technique may not lend selectivity to the detection of NO_2 against other oxidizing chemicals such as Cl_2 and ozone, and much work is still needed to improve the selectivity.

In summary, the NO_2 sensing property of In_2O_3 nanowire-based nanosensors was systematically studied. The single In_2O_3 nanowire sensors showed a detection limit of ~20 ppb, which is the lowest detectable concentration ever achieved with all types of metal oxide nanowire sensors and all conventional solid-state NO_2 sensors working at room temperature. Furthermore, we have also developed and investigated the multiwire device structure, which has been demonstrated as a more reliable and sensitive NO_2 sensor compared to the single-wire devices. An even lower detection limit of 5 ppb has been achieved. The highly selective sensing to NH_3 and NO_2 gas can be understood by the "averaging" mechanism in the multiwire sensors.

References

(1) Xia, Y. N.; Yang, P. D.; Sun, Y. G.; Wu, Y. Y.; Mayers, B.; Gates, B.; Yin, Y. D.; Kim, F.; Yan, Y. Q. *Adv. Mater.* **2003**, *15*, 353−389.
(2) Kong, J.; Franklin, N. R.; Zhou, C. W.; Chapline, M. G.; Peng, S.; Cho, K. J.; Dai, H. J. *Science* **2000**, *287*, 622−625.
(3) Qi, P.; Vermesh, O.; Grecu, M.; Javey, A.; Wang, Q.; Dai, H. J. *Nano. Lett.* **2003**, *3*, 347−351.
(4) Li, J.; Lu, Y.; Cinke, M.; Han, J.; Meyyappan, M. *Nano. Lett.* **2003**, *3*, 929−933.
(5) Law, M.; Kind, H.; Messer, B.; Kim, F.; Yang, P. D. *Angew. Chem., Int. Ed.* **2002**, *41*, 2405−2408.
(6) Li, C.; Zhang, D. H.; Liu, X. L.; Han, S.; Tang, T.; Han, J.; Zhou, C. W. *Appl. Phys. Lett.* **2002**, *82*, 1613−1615.
(7) Comini, E.; Faglia, G.; Sberveglieri, G.; Pan, Z. W.; Wang, Z. L. *Appl. Phys. Lett.* **2002**, *81*, 1869−1871.
(8) Huang, J. X.; Virji, S.; Weiller, B. H.; Kaner, R. B. *J. Am. Chem. Soc.* **2003**, *125*, 314−315.
(9) Murray, B. J.; Walter, E. C.; Penner, R. M. *Nano Lett.* **2004**, *4*, 665−670.
(10) Kolmakov, A.; Zhang, Y. X.; Cheng, G. S.; Moskovits, M. *Adv. Mater.* **2003**, *15*, 997−1000.
(11) Liu, H. Q.; Kameoka, J.; Czaplewski, D. A.; Craighead, H. G. *Nano Lett.* **2004**, *4*, 671−675.
(12) U. S. environmental protection agency, "Air Trends Summary Report", http://www.epa.gov/oar/aqtrnd95/no2.html.
(13) Shieh, J.; Feng, H. M.; Hon, M. H.; Juang, H. Y. *Sens. Actuators B* **2002**, *86*, 75−80.
(14) Winter, R.; Scharnagl, K.; Fuchs, A.; Doll, T.; Eisele, I. *Sens. Actuators B* **2000**, *66*, 85−87.
(15) Steffes, H.; Imawan, C.; Solzbacher, F.; Obermeier, E. *Sens. Actuators B* **2001**, *78*, 106−112.
(16) Jones, T. A.; Bott, B. *Sens. Actuators* **1986**, *9*, 27−37.

(17) Xie, D.; Jiang, Y.; Pan, W.; Li, D.; Wu, Z.; Li, Y. *Sens. Actuators B* **2003**, *90*, 163−169.

(18) Li, C.; Zhang, D. H.; Han, S.; Liu, X. L.; Tang, T.; Zhou, C. W. *Adv. Mater.* **2003**, *15*, 143−146.

(19) We note that even though Langmuir isotherm describes gas adsorption at equilibrium, the normalized conductance change in this study is calculated from the device conductance before and after 20-minute NO$_2$ exposure, which was sufficiently long for the system to reach quasi equilibrium.

(20) Comini, E.; Guidi, V.; Malagu, C.; Martinelli, G.; Pan, Z.; Shervuglieri, G.; Wang, Z. L. *J. Phys. Chem. B* **2004**, *108*, 1882.

(21) Zhang, D. H.; Li, C.; Liu, X. L.; Han, S.; Tang, T.; Zhou, C. W. *Appl. Phys. Lett.* **2003**, *83*, 1845−1847.